Flow Development in the Hydrodynamic Entrance Region of a Flat Duct

R. C. GUPTA

Indian Institute of Technology, Kanpur, India

Recently, Campbell and Slattery (2) have studied the developing flow of an incompressible Newtonian fluid in the entrance region of a tube. They have corrected Shiller's solution to account for the loss of energy due to viscous dissipation in the boundary layer. We made a similar study of the flow behavior in the entrance of a flat duct. It is believed that the results will provide a better description of the flow, because here we applied macroscopic mechanical energy balance (Bernoulli equation) to all the fluid in the duct instead of applying it only to the nonviscous core. Furthermore, this approach showed that the fully developed results are reached asymptotically as predicted by various developments, although solutions based on Shiller's approach fail in this respect.

ANALYSIS

We considered the laminar flow of an incompressible Newtonian fluid entering a duct, formed by two horizontal semi-infinite plates spaced a distance $2h$ apart with uniform velocity.

The macroscopic mass balance (1) may be applied between $x = 0$ (the entry) and an arbitrary cross section x to give

$$Q = 2\int_o^h u\,dy \tag{1}$$

Following Shiller, we assumed the boundary-layer velocity profile to be of the form

$$u = U\left[\,1 - \left(1 - \frac{h-y}{\delta}\right)^2\,\right] \tag{2}$$

Then (1) may be written as

$$Q = 2\int_o^{h-\delta} U\,dy + 2\int_{h-\delta}^{h} u\,dy \tag{3}$$

This simplifies to

$$\frac{Q}{2Uh} = 1 - \frac{1}{3}\cdot\frac{\delta}{h} \tag{4}$$

The macroscopic momentum balance (or integrated equation of motion) may be written as (1)

$$\Delta(\rho\langle u^2\rangle S + pS) + F_{drag} = 0 \tag{5}$$

By applying this to the differential length dx, we obtain

$$\rho\frac{d}{dx}\int_o^h u^2dy + h\frac{dp}{dx} + T_{xy}\big|_{y=h} = 0, \tag{6}$$

where

$$T_{xy}\big|_{y=h} = -\mu\left.\frac{\partial u}{\partial y}\right|_{y=h} = 2\mu\frac{U}{\delta} \tag{7}$$

The macroscopic mechanical energy balance may be written as (1)

$$\Delta\left(\frac{1}{2}\rho S\langle u^3\rangle\right) + w\int_{p_1}^{p_2}\frac{dp}{\rho} + E_v = 0 \tag{8}$$

The assumption that the square of the velocity in the axial direction is much larger than the sum of the squares of all other velocity components is incorporated in Equation (8). By applying Equation (8) to the fluid between the entry and an arbitrary cross section, we obtain

$$\frac{1}{2}\rho\int_o^h u^3dy - \frac{1}{2}\rho V^2h + p\int_o^h u\,dy - p_oVh + E_v = 0 \tag{9}$$

Total rate of viscous dissipation of energy is given by

$$E_v = \int_o^x\int_o^h \mu\left(\frac{\partial u}{\partial y}\right)^2 dx\,dy \tag{10}$$

By differentiating Equation (9) with respect to x after eliminating E_v, we obtain

$$\frac{Q}{2}\frac{dp}{dx} = -\frac{1}{2}\rho\frac{d}{dx}\int_o^h u^3dy - \mu\int_o^h\left(\frac{\partial u}{\partial y}\right)^2 dy \tag{11}$$

We now eliminate $\dfrac{dp}{dx}$, u, and U between (2), (4), (6), and (11) to give after simplification

$$1120\,x^* = \Big[\,196\,\delta^* - 17\ln(1-\delta^*) + 1233\ln(3-\delta^*) + \frac{1782}{(3-\delta^*)}\,\Big]_o^{\delta^*} \tag{12}$$

This relates the dimensionless distance from the entry to the dimensionless boundary-layer thickness.

The relation between the pressure drop and the boundary-layer thickness can be obtained either from (6) or (9). The dimensionless entrance length pressure distribution is found to be given by

$$140\,p^* = 3\left[\,17\ln\left(\frac{3-\delta^*}{1-\delta^*}\right) - \frac{34}{3-\delta^*} + \frac{258}{(3-\delta^*)^2}\,\right]_o^{\delta^*} \tag{13}$$

Equations (12) and (13) give p^* at any x^*.

The velocity U in the central core can be determined from (4) and is given by

$$\frac{U}{V} = \frac{1}{1-\frac{1}{3}\delta^*} \tag{14}$$

The boundary-layer velocity profile can be obtained from (2) and (14) as

$$u = \frac{V}{\left(1-\frac{1}{3}\delta^*\right)}\left[\,1 - \left(1 - \frac{1-\frac{y}{h}}{\delta^*}\right)^2\,\right] \tag{15}$$

Nonlinear least squares analysis of catalytic rate models, Kittrell, J. R., W. G. Hunter, and C. C. Watson, **A.I.Ch.E. Journal, 11,** No. 6, p. 1051 (November, 1965).

Key Words: A. Catalysis-8, Heterogeneous-0, Least Squares-10, Linear-0, Nonlinear-0, Reactor-10, 9, Design-4, Temperature-6, Partial Pressure-6, Reaction Rate-1, 7, Nitric Oxide-1, Hydrogen-1, Nitrogen-2, Water-2, Ammonia-3, Zinc-10, Copper-10, Chromia-10, Catalyst-10, Design-8, Analysis-8, Models-2, 8, 9, Computer-10, Rate Equation-2, Experimental-0.

Abstract: Conventional data generation and analysis procedures used to select a descriptive Hougen-Watson reaction rate model are reviewed and some statistical objections to these conventional procedures are presented. The gaseous reaction considered was the reduction of nitric oxide: $NO + H_2 \rightleftharpoons H_2O + 1/2\ N_2$. Comparisons are made between the results of the conventional linear least squares analysis of isothermal data and those of nonlinear least squares analyses of both isothermal and nonisothermal data. It was found that the nonlinear least squares procedures were useful for a rational selection of an acceptable model and estimation of its parameters.

Chemical reaction in the turbulent wake of a cylinder, Saidel, G. M., and H. E. Hoelscher, **A.I.Ch.E. Journal, 11,** No. 6, p. 1058 (November, 1965).

Key Words: A. Turbulence-6, Rate-7, Chemical Reaction-9, 7, Wake-9, Cylinder-9.

Abstract: In this paper an experimental study of rapid, irreversible, second-order reactions in the turbulent wake of a cylinder is described. The effect of the turbulence on the reaction rate was studied. The main objective of the experiments was to obtain the mean concentration of one reactant as a function of position with and without another reactant present. In addition experiments were made to compare the reaction process occurring within the turbulent core with the reaction process occurring throughout the wake.

Laminar dispersion in capillaries: Part I. Mathematical analysis, Ananthakrishnan, V., W. N. Gill, and A. J. Barduhn, **A.I.Ch.E. Journal, 11,** No. 6, p. 1063 (November, 1965).

Key Words: A. Laminar-0, Dispersion-8, 7, Peclet Number-6, Time-6, Distance-6, Radius-9, Axis-9, Concentration-7, Finite Difference-10, Tube-9, Diffusion-8, 7, Taylor-Aris Theory-8, Capillaries-9, Mathematics-10.

Abstract: Laminar dispersion in tubes is studied and it is shown that the Taylor-Aris theory is valid for sufficiently large values of τ (dimensionless time). Axial molecular diffusion is significant at low N_{Pe} but the magnitude of N_{Pe} at which this occurs depends on the value of τ.

Simple expressions were developed empirically for the average concentration distribution which apply over wider ranges of N_{Pe} and τ than previously reported expressions.

Evaporation from falling saline water films in laminar transitional flow, Unterberg, Walter, and D. K. Edwards, **A.I.Ch.E. Journal, 11,** No. 6, p. 1073 (November, 1965).

Key Words: A. Evaporation-8, Films-9, Water-9, Saline Water-9, Surface-9, Vertical-0, Continuity-8, Boiling Point Elevation-8, Laminar Flow-9, Transitional Flow-9.

Abstract: An analytical and experimental study was made of the evaporation from pure and saline water films flowing down a heated vertical surface at Reynolds numbers between 160 and 600. Visual observation showed free surface evaporation. Film continuity was poor for pure water, but good for saline water, owing to the influence of temperature and salinity on surface tension gradients. Evaporation rates were predicted by three theories: a constant-property, boundary-layer type of laminar analysis; the constant-property Dukler eddy treatment; and a variable-property laminar analysis which took into account the boiling point elevation due to salinity. The experimental evaporation rates could be correlated by dimensionless moduli arising out of the laminar analyses, but best quantitative agreement was found with the Dukler eddy treatment.

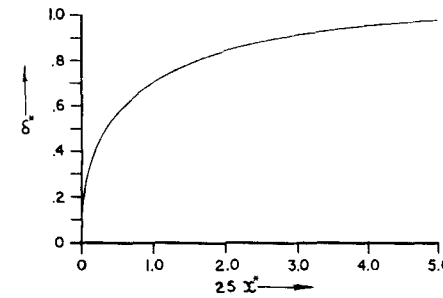

Fig. 1. Boundary-layer thickness vs. axial position.

For any given x^*, Equations (12) and (15) determine the velocity profile in the boundary layer. Outside the boundary layer, that is, in the accelerated zone, the velocity profile is a straight line, since the velocity is constant there.

Figures 1 and 2 show the variations of δ^* and p^* with x^*. Boundary-layer velocity profiles, velocity as a function of location in the entrance region, and velocity in the core region can be plotted very easily with Equations (2) and (14).

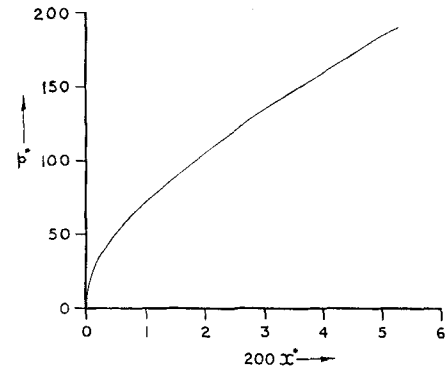

Fig. 2. Entrance length pressure distribution.

ACKNOWLEDGMENT

The author wishes to express his sincere and heartfelt thanks to Dr. J. N. Kapur, Indian Institute of Technology, Kanpur, for the inspiration and guidance during the work.

NOTATION

E_v = total rate of dissipation of energy
F_{drag} = force exerted by the fluid on the duct walls
$2h$ = channel width
N_{Re} = Reynolds number, $4\rho Vh/\mu$
p = pressure
p_o = pressure at the entry
p^* = dimensionless pressure drop, $(p_o-p)/\frac{1}{2}\rho V^2$
Q = volume rate of flow through the channel
S = cross-sectional area for the flow

u, v = velocities in the boundary layer in x and y directions, respectively
U = velocity of the fluid in the central core
V = average velocity, $Q/2h$
x, y = Cartesian coordinates
x^* = dimensionless axial distance, $x/h\,N_{Re}$
w = mass rate of flow

Greek Letters

δ = boundary-layer thickness
δ^* = dimensionless boundary-layer thickness, δ/h
μ = viscosity
ρ = density
$< >$ = average over cross section available for flow of quantity enclosed
$\Delta( )$ = difference of the quantity enclosed at an arbitrary cross section and at the entry

LITERATURE CITED

1. Bird, R. B., W. E. Stewart, and E. N. Lightfoot, "Transport Phenomena," Wiley, New York (1962).
2. Campbell, W. D., and J. C. Slattery, *Trans. Am. Soc. Mech. Engrs.*, **85D**, 41-44 (1963).

Investigation of Heat Transfer to Liquid Metals Flowing in Circular Tubes

ROBERT E. HOLTZ

Argonne National Laboratory, Argonne, Illinois

In a recent article, Dwyer (*1*) has discussed the heating and cooling of turbulent flowing liquids in circular tubes. A result of this analysis is that the equation

$$N_{Nu} = 7.0 + 0.025 \left[N_{Pe} - \frac{1.82\,N_{Re}}{(\epsilon_M/\nu)^{1.4}_{\max}} \right]^{0.8} \quad (1)$$

could be utilized to estimate heat transfer rates to liquid metals flowing in circular tubes under fully established flow and constant heat flux conditions. Equation (1) applies for Peclet numbers above the critical Peclet number. Below the critical Peclet number it is recommended that the Nusselt number be assumed equal to 7.0. The critical Peclet number is defined as that Peclet number corresponding to the highest Reynolds number, for a given Prandtl number, at which heat is transferred by molecular conduction only.

The results of Lyon (*2*) in an earlier study indicate that the semi-empirical relationship

$$N_{Nu} = 7.0 + 0.025\,(N_{Pe})^{0.8} \quad (2)$$

may be utilized to estimate heat transfer coefficients under turbulent flow and uniform heat input conditions for liquid metals flowing in tubes.

Equations (1) and (2) are in fair agreement with each other. Recent data from the Brookhaven National Laboratory (*3*) appear to be in reasonable agreement with both expressions.

Other investigators have reported lower results. Lubarsky and Kaufman (*4*) have presented the expression

$$N_{Nu} = 0.625\,N_{Pe}^{0.4} \quad (3)$$

for fully developed turbulent heat transfer to liquid metals flowing in tubes. Reference 5 discusses the various effects which contribute to the disagreement of experimental measured liquid-metal heat transfer coefficients.

In the laminar flow region, the Nusselt number should equal 4.4 (*1*). This is in agreement with the experimental results of Petukhov and Yushin (*6*).

The purpose of this communication is to report information gained in an experiment in which a constant heat flux was supplied to liquid sodium-potassium flowing vertically in a circular tube. Data obtained from this experiment are in the laminar, transition, and turbulent regions.

EXPERIMENTAL APPARATUS

A schematic diagram of the experimental loop is shown in Figure 1. The loop was constructed primarily of 0.500 in. O.D., 0.035 in. wall, type 316 stainless steel and was contained within an evacuated enclosure. Sodium-potassium alloy (NaK-78) was used as the heat transfer fluid. The loop contained a 16-in. long thermal radiation heated test section. Radiation shields surrounded the heated section to reduce heat losses. Heat was removed from the loop by means of a cooling coil designed to remove heat by thermal radiation. An electromagnetic pump was used for circulating the sodium-potassium and an e.m. flowmeter was used for obtaining flow rates. Chromel-alumel thermocouples were employed to measure temperatures at key points in the system. The loop was pressurized by utilizing an argon gas blanket on the sodium-potassium surface in the dump tank.

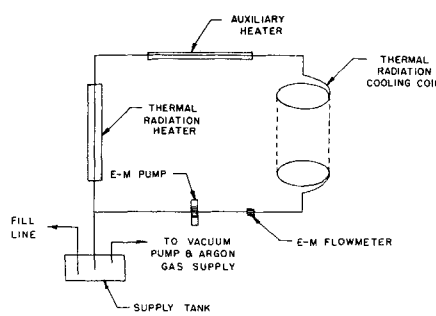

Fig. 1. Schematic diagram of thermal radiation heated loop.

The vertical thermal radiation heated test section consisted of a 0.500-in. O.D., 0.035-in. wall, type 316 stainless steel tube containing the flowing sodium-potassium. The tube was surrounded by two half cylindrical shaped tantalum elements which were 16 in. long and electrically heated. The test section had an L/D ratio of 37. Heat was transferred from the 0.003-in. thick heating elements to the tube containing the flowing sodium-potassium by thermal radiation. The heat was then conducted through the tube wall to the liquid sodium-potassium.

The heat flux was determined both by utilizing an energy balance on the sodium-potassium passing through the thermal radiation heater and from power measurements less calculated losses. These two techniques for determining the heat flux showed excellent agreement (within ± 4%). The heat flux was uniform along the heated length except for a sharp decrease within approximately 1 in. of both the heater inlet and heater outlet.

Two chromel-alumel thermocouples were located both at the inlet and at the outlet of the heated section to measure the sodium-potassium temperature at these points. These thermocouples were located several inches from both the actual heater inlet and heater outlet to eliminate any heater end effects upon the thermocouple readings and to assure proper mixing of the fluid at the heater outlet. With the inlet and outlet temperatures and heat flux known, the bulk fluid temperature was determined as a function of length along the vertical heater. Three chromel-alumel thermocouples were spot welded to the outside tube wall in the middle of